Algorithm-based Fault Tolerance for Dense Matrix Factorizations

Peng Du Aurelien Bouteiller George Bosilca Thomas Herault Jack Dongarra

Innovative Computing Laboratory, University of Tennessee, Knoxville
{du,bouteill,bosilca,herault,dongarra}@eecs.utk.edu

Abstract

Dense matrix factorizations, such as LU, Cholesky and QR, are widely used for scientific applications that require solving systems of linear equations, eigenvalues and linear least squares problems. Such computations are normally carried out on supercomputers, whose ever-growing scale induces a fast decline of the Mean Time To Failure (MTTF). This paper proposes a new hybrid approach, based on Algorithm-Based Fault Tolerance (ABFT), to help matrix factorizations algorithms survive fail-stop failures. We consider extreme conditions, such as the absence of any reliable component and the possibility of loosing both data and checksum from a single failure. We will present a generic solution for protecting the right factor, where the updates are applied, of all above mentioned factorizations. For the left factor, where the panel has been applied, we propose a scalable checkpointing algorithm. This algorithm features high degree of checkpointing parallelism and cooperatively utilizes the checksum storage leftover from the right factor protection. The fault-tolerant algorithms derived from this hybrid solution is applicable to a wide range of dense matrix factorizations, with minor modifications. Theoretical analysis shows that the fault tolerance overhead sharply decreases with the scaling in the number of computing units and the problem size. Experimental results of LU and QR factorization on the Kraken (Cray XT5) supercomputer validate the theoretical evaluation and confirm negligible overhead, with- and without-errors.

Categories and Subject Descriptors G.4 [*Mathematical Software*]: Reliability and robustness

General Terms Algorithms

Keywords ABFT, Fault-tolerance, Fail-stop failure, LU, QR

1. Introduction

Today's high performance computers have paced into Petaflops realm, through the increase of system scale. The number of system components, such as CPU cores, memory, networking, and storage grow considerably. One of the most powerful Petaflop scale machines, Kraken [2], from National Institute for Computational Sciences and University of Tennessee, harnessed as many as 112,800 cores to reach its peak performance of 1.17 Petaflops to rank No.11 on the November 2011 Top500 list. With the increase of system scale and chip density, the reliability and availability of such systems has declined. It has been shown that, under specific circumstances, adding computing units might hamper applications completion time, as a larger node count implies a higher probability of reliability issues. This directly translates into a lower efficiency of the machine, which equates to a lower scientific throughput [24]. It is estimated that the MTTF of High Performance Computing (HPC) systems might drop to about one hour in the near future [7]. Without a drastic change at the algorithmic level, such a failure rate will certainly prevent capability applications from progressing.

Exploring techniques for creating a software ecosystem and programming environment capable of delivering computation at extreme scale, that are both resilient and efficient, will eliminate a major obstacle to scientific productivity on tomorrow's HPC platforms. In this work we advocate that in extreme scale environments, successful approaches to fault tolerance (e.g. those which exhibit acceptable recovery times and memory requirements) must go beyond traditional systems-oriented techniques and leverage intimate knowledge of dominant application algorithms, in order to create a middleware that is far more adapted and responsive to the application's performance and error characteristics.

While many types of failures can strike a distributed system [16], the focus of this paper is on the most common representation: the fail-stop model. In this model, a failure is defined as a process that *completely* and *definitely* stops responding, triggering the loss of a critical part of the global application state. To be more realistic, we assume a failure could occur at any moment and can affect any parts of the application's data. We introduce a new generic hybrid approach based on algorithm-based fault tolerance (ABFT) that can be applied to several ubiquitous one-sided dense linear factorizations. Using one of these factorizations, namely LU with partial pivoting, which is significantly more challenging due to pivoting, we theoretically prove that this scheme successfully applies to the three well known one-sided factorizations, Cholesky, LU and QR. To validate these claims, we implement and evaluate this generic ABFT scheme with both the LU and QR factorizations. A significant contribution of this work is to protect the part of the matrix below the diagonal (referred to as "the left factor" in the rest of the text) during the factorization, which was hitherto never achieved.

The rest of the paper is organized as follows: Section 2 presents background and prior work in the domain; Section 3 reviews the features of full factorizations. Section 4 discusses the protection of the right factor using the ABFT method. Section 5 reviews the idea of vertical checkpointing and proposes the new checkpointing method to protect the left factor. Section 6 evaluates the performance and overhead of the proposed algorithm using the example of LU and QR, and section 7 concludes the work.

PPoPP'12, February 25–29, 2012, New Orleans, Louisiana, USA.

2. Algorithm Based Fault Tolerance Background

The most well-known fault-tolerance technique for parallel applications, checkpoint-restart (C/R), encompasses two categories, the system and application level. At the system level, message passing middleware deals with faults automatically, without intervention from the application developer or user ([5, 6]). At the application level, the application state is dumped to a reliable storage when the application code mandates it. Even though C/R bears the disadvantage of high overhead while writing data to stable storage, it is widely used nowadays by high end systems [1]. To reduce the overhead of C/R, diskless checkpointing [21, 23] has been introduced to store checksum in memory rather than stable storage. While diskless checkpointing has shown promising performance in some applications (for instance, FFT in [14]), it exhibits large overheads for applications modifying substantial memory regions between checkpoints [23], as is the case with factorizations.

In contrast, Algorithm Based Fault Tolerance (ABFT) is based on adapting the algorithm so that the application dataset can be recovered at any moment, without involving costly checkpoints. ABFT was first introduced to deal with silent error in systolic arrays [19]. Unlike other methods that treat the recovery data and computing data separately, ABFT approaches are based on the idea of maintaining consistency of the recovery data, by applying appropriate mathematical operations on both the original and recovery data. Typically, for linear algebra operations, the input matrix is extended with supplementary columns and/or rows containing checksums. This initial encoding happens only once; the matrix algorithms are designed to work on the encoded checksum along with matrix data, similar mathematical operations are applied to both the data and the checksum so that the checksum relationship is kept invariant during the course of the algorithm. Should some data be damaged by failures, it is then possible to recover the application by inverting the checksum operation to recreate missing data. The overhead of ABFT is usually low, since no periodical global checkpoint or rollback-recovery is involved during computation and the computation complexity of the checksum operations scales similarly to the related matrix operation. ABFT and diskless checkpointing have been combined to apply to basic matrix operations like matrix-matrix multiplication [4, 8–10] and have been implemented on algorithms similar to those of ScaLAPACK [3], which is widely used for dense matrix operations on parallel distributed memory systems.

Recently, ABFT has been applied to the High Performance Linpack (HPL) [12] and to the Cholesky factorization [18]. Both Cholesky and HPL have the same factorization structure, where only half of the factorization result is required, and the update to the trailing matrix is based on the fact that the left factor result is a triangular matrix. This approach however does not necessarily apply to other factorizations, like QR where the left factor matrix is full, nor when the application requires both the left and right factorization results. Also, LU with partial pivoting, when applied to the lower triangular L, potentially changes the checksum relation and renders basic checkpointing approaches useless.

The generic ABFT framework for matrix factorizations we introduce in this work can be applied not only to Cholesky and HPL, but also to LU and QR. The right factor is protected by a traditional ABFT checksum, while the left factor is protected by a novel vertical checkpointing scheme, making the resulting approach an hybrid between ABFT and algorithm driven checkpointing. Indeed, this checkpointing algorithm harnesses some of the properties of the factorization algorithm to exchange limited amount of rollback with the ability to overlap the checkpointing of several panel operations running in parallel. Other contributions of this work include correctness proofs and overhead characterization for the ABFT approach on the most popular 2D-block cyclic distribution (as opposed to the 1D distributions used in previous works). These proofs consider the effect of failures during critical phases of the algorithm, and demonstrate that recovery is possible without suffering from error propagation

3. Full Factorizations of Matrix

In this work, we consider the case of factorizations where the lower triangular part of the factorization result matters, as is the case in QR and LU with pivoting. For example, the left factor Q is required when using QR to solve the least square problem, and so is L when solving $A^k x = b$ with the "LU factorization outside the loop" method [17]. In the remaining of this section, we recall the main algorithm of the most complex case of one-sided factorization, block LU with pivoting. Additionally, we highlight challenges specific to this type of algorithms, when compared to algorithms studied in previous works.

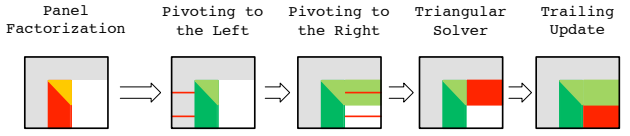

Figure 1. Steps applied to the input matrix in an iteration of the LU factorization; Green: Just finished; Red & Orange: being processed; Gray: Finished in previous iterations

Figure 1 presents the diagram of the basic operations applied to the input matrix to perform the factorization. The block LU factorization algorithm can be seen as a recursive process. At each iteration, the panel factorization is applied on a block column. This panel operation factorizes the upper square (selecting adequate pivots and applying internal row swapping as necessary to ensure numerical stability), and scales the lower polygon accordingly. The output of this panel is used to apply row swapping to the result of previous iterations, on the left, and to the trailing matrix on the right. The triangular solver is applied to the right of the factored block to scale it accordingly, and then the trailing matrix is updated by applying a matrix-matrix multiply update. Then the trailing matrix is used as the target for the next iteration of the recursive algorithm, until the trailing matrix is empty. Technically, each of these basic steps is usually performed by applying a parallel Basic Linear Algebra Subroutine (PBLAS).

The structure of the other one-sided factorizations, Cholesky and QR, are similar with minor differences. In the case of Cholesky, the trailing matrix update involves only the upper triangle, as the lower left factor is not critical. For QR, the computation of pivots and the swapping are not necessary as the QR algorithm is more stable. Moreover, there are a significant number of applications, like iterative refinement and algorithms for eigenvalue problems, where the entire factorization result, including the lower part, is needed. Therefore, a scalable and efficient protection scheme for the lower left triangular part of the factorization result is required.

4. Protection of the Right Factor Matrix with ABFT

In this section, we detail the ABFT approach that is used to protect the upper triangle from failures, while considering the intricacies of typical block cyclic distributions and failure detection delays.

4.1 Checksum Relationship

ABFT approaches are based upon the principle of keeping an invariant bijective relationship between protective supplementary

blocks and the original data through the execution of the algorithm, by the application of numerical updates to the checksum. In order to use ABFT for matrix factorization, an initial checksum is generated before the actual computation starts. In future references we use G to refer to the generator matrix, and A to the original input matrix. The checksum C for A is produced by

$$C = GA \text{ or } C = AG \tag{1}$$

When G is all-1 vector, the checksum is simply the sum of all data items from a certain row or column. Referred to as the *checksum relationship*, (1) can be used at any step of the computation for checking data integrity (by detecting mismatching checksum and data) and recovery (inverting the relation builds the difference between the original and the degraded dataset). With the type of failures we consider (Fail-Stop), data cannot be corrupted, so we will use this relationship to implement the recovery mechanism only. This relationship has been shown separately for Cholesky [18], and HPL [12], both sharing the property of updating the trailing matrix with a lower triangular matrix. However, in this work we consider the general case of matrix factorization algorithms, including those where the full matrix is used for trailing matrix updates (as is the case for QR and LU with partial pivoting). In this context, the invariant property has not been demonstrated; we will now demonstrate that it holds for full matrix based updates algorithms as well.

4.2 Checksum Invariant with Full Matrix Update

In [22], ZU is used to represent a matrix factorization (optionally with pairwise pivoting for LU), where Z is the left matrix (lower triangular in the case of Cholesky or full for LU and QR) and U is an upper triangular matrix. The factorization is then regarded as the process of applying a series of matrices Z_i to A from the left until $Z_i Z_{i-1} \cdots Z_0 A$ becomes upper triangular.

Theorem 4.1. *Checksum relationship established before ZU factorization is maintained during and after factorization.*

Proof. Suppose data matrix $A \in \mathbb{R}^{n \times n}$ is to be factored as $A = ZU$, where $Z \text{ and } U \in \mathbb{R}^{n \times n}$ and U is an upper triangular matrix. A is checkpointed using generator matrix $G \in \mathbb{R}^{n \times nc}$, where nc is the width of checksum. To factor A into upper triangular form, a series of transformation matrices Z_i is applied to A (with partial pivoting in LU).

Case 1: No Pivoting

$$U = Z_n Z_{n-1} \dots Z_1 A \tag{2}$$

Now the same operation is applied to $A_c = [A,\ AG]$

$$\begin{aligned} U_c &= Z_n Z_{n-1} \dots Z_1 [A,\ AG] \\ &= [Z_n Z_{n-1} \dots Z_1 A,\ \ Z_n Z_{n-1} \dots Z_1 AG] \\ &= [U,\ UG] \end{aligned} \tag{3}$$

For any $k \leq n$, using U^k to represent the result of U at step k,

$$\begin{aligned} U_c^k &= Z_k Z_{k-1} \dots Z_1 [A,\ AG] \\ &= [Z_k Z_{k-1} \dots Z_1 A,\ \ Z_k Z_{k-1} \dots Z_1 AG] \\ &= \left[U^k,\ U^k G\right] \end{aligned} \tag{4}$$

Case 2: With partial pivoting:

$$\begin{aligned} U_c^k &= Z_k P_k Z_{k-1} P_{k-1} \dots Z_1 P_1 [A,\ AG] \\ &= [Z_k P_k Z_{k-1} P_{k-1} \dots Z_1 P_1 A, \\ &\qquad Z_k P_k Z_{k-1} P_{k-1} \dots Z_1 P_1 AG] \\ &= \left[U^k,\ U^k G\right] \end{aligned} \tag{5}$$

Therefore the checksum relationship holds for LU with partial pivoting, Cholesky and QR factorizations. □

4.3 Checksum Invariant in Block Algorithms

Theorem 4.1 shows the mathematical checksum relationship in matrix factorizations. However, in real-world, HPC factorizations are performed in block algorithms, and execution is carried out in a recursive way. Linear algebra packages, like ScaLAPACK, consist of several function components for each factorization. For instance, LU has a panel factorization, a triangular solver and a matrix-matrix multiplication. We need to ensure that the checksum relationship also holds for block algorithms, both at the end of each iteration, and after the factorization is completed.

Theorem 4.2. *For ZU factorization in block algorithm, checksum at the end of each iteration only covers the upper triangular part of data that has already been factored and are still being factored in the trailing matrix.*

Proof. Input Matrix A is split into blocks of data of size $nb \times nb$ (A_{ij}, Z_{ij}, U_{ij}), and the following stands:

$$\begin{bmatrix} A_{11} & A_{12} & A_{13} \\ A_{21} & A_{22} & A_{23} \end{bmatrix} = \begin{bmatrix} Z_{11} & Z_{12} \\ Z_{21} & Z_{22} \end{bmatrix} \begin{bmatrix} U_{11} & U_{12} & U_{13} \\ 0 & U_{22} & U_{23} \end{bmatrix}, \tag{6}$$

where $A_{13} = A_{11} + A_{12}$, and $A_{23} = A_{21} + A_{22}$.

Since $A_{13} = Z_{11}U_{13} + Z_{12}U_{23}$, and $A_{23} = Z_{21}U_{13} + Z_{22}U_{23}$, and using the relation

$$\begin{cases} A_{11} &= Z_{11}U_{11} \\ A_{12} &= Z_{11}U_{12} + Z_{12}U_{22} \\ A_{21} &= Z_{21}U_{11} \\ A_{22} &= Z_{21}U_{12} + Z_{22}U_{22} \end{cases}$$

in (6), we have the following system of equations:

$$\begin{cases} Z_{21}(U_{11} + U_{12} - U_{13}) = Z_{22}(U_{23} - U_{22}) \\ Z_{11}(U_{11} + U_{12} - U_{13}) = Z_{12}(U_{23} - U_{22}) \end{cases}$$

This can be written as:

$$\begin{bmatrix} Z_{11} & Z_{12} \\ Z_{21} & Z_{22} \end{bmatrix} \begin{bmatrix} U_{11} + U_{12} - U_{13} \\ -(U_{23} - U_{22}) \end{bmatrix} = 0$$

For LU, Cholesky and QR, $\begin{bmatrix} Z_{11} & Z_{12} \\ Z_{21} & Z_{22} \end{bmatrix}$ is always nonsingular, so $\begin{bmatrix} U_{11} + U_{12} - U_{13} \\ U_{23} - U_{22} \end{bmatrix} = 0$, and $\begin{cases} U_{11} + U_{12} &= U_{13} \\ U_{23} &= U_{22} \end{cases}$.

This shows that after ZU factorization, checksum blocks cover the upper triangular matrix U only, even for the diagonal blocks. At the end of each iteration, for example the first iteration in (6), Z_{11}, U_{11}, Z_{21} and U_{12} are completed, and U_{13} is already $U_{11} + U_{12}$. The trailing matrix A_{22} is updated with

$$A_{22}{}' = A_{22} - Z_{21}U_{12} = Z_{22}U_{22}.$$

and A_{23} is updated to

$$\begin{aligned} A_{23}{}' &= A_{23} - Z_{21}U_{13} \\ &= A_{21} + A_{22} - Z_{21}(U_{11} + U_{12}) \\ &= Z_{21}U_{11} + A_{22} - Z_{21}U_{11} - Z_{21}U_{12} \\ &= A_{22} - Z_{21}U_{12} = Z_{22}U_{22} \end{aligned}$$

Therefore, at the end of each iteration, data blocks that have already been and are still being factored remain covered by checksum blocks. □

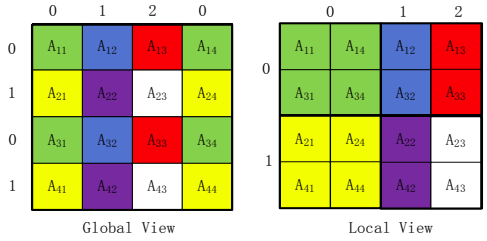

Figure 2. Example of a 2D block-cyclic data distribution

4.4 Issues with Two-Dimensional Block-cyclic Distribution

It has been well established that data layout plays an important role in the performance of parallel matrix operations on distributed memory systems [11, 20]. In 2D block-cyclic distributions, data is divided into equally sized blocks, and all computing units are organized into a virtual two-dimension grid P by Q. Each data block is distributed to computing units in round robin following the two dimensions of the virtual grid. Figure 2 is an example of a $P = 2, Q = 3$ grid applied to a global matrix of 4×4 blocks. The same color represents the same process while numbering in A_{ij} indicates the location in the global matrix. This layout helps with load balancing and reduces data communication frequency, because in each step of the algorithm, many computing units can be engaged in computations concurrently, and communications pertaining to blocks positioned on the same unit can be grouped. Thanks to these advantages, many prominent software libraries (like ScaLAPACK [13]) assume a 2D block-cyclic distribution.

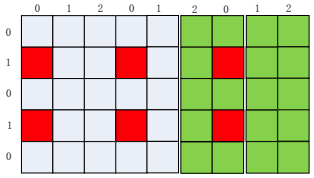

Figure 3. Holes in a checksum protected matrix caused by a single failure and the naive checksum duplication protection scheme (3x2 process grid)

However, with a 2D block-cyclic data distribution, the failure of a single process, usually a computing node which keeps several non-contiguous blocks of the matrix, results in holes scattered across the whole matrix. Figure 3 is an example of a 5×5 blocks matrix (on the left) with a 2×3 process grid. Red blocks represent holes caused by the failure of the single process (1, 0). In the general case, these holes can impact both checksum and matrix data at the same time.

4.5 Checksum Protection Against Failure

Our algorithm works under the assumption that any process can fail and therefore the data, including the checksum, can be lost. Rather than forcing checksum and data on different processes and assuming only one would be lost, as in [12], we put checksum and data together in the process grid and design the checksum protection algorithm accordingly.

4.5.1 Minimum Checksum Amount for Block Cyclic Distributions

Theoretically, the sum-based checksum C_k of a series of N blocks $A_i, 1 \leq i \leq N$, where N is the total number of blocks in one row/column of the matrix, is computed by:

$$C_k = \sum_{k=1}^{N} A_k \tag{7}$$

With the 2D block-cyclic distribution, a single failure punches multiple holes in the global matrix. With more than one hole per row/column, C_k in (7) is not sufficient to recover all lost data. A slightly more sophisticated checksum scheme is required.

Theorem 4.3. *Using sum-based checkpointing, for N data items distributed in block-cyclic onto Q processes, the size of the checksum to recover from the loss of one process is $\lceil \frac{N}{Q} \rceil$*

Proof. With 2D block-cyclic, each process gets $\lceil \frac{N}{Q} \rceil$ items. At the failure of one process, all data items in the group held by the process are lost. Take data item a_i, $1 \leq i \leq \lceil \frac{N}{Q} \rceil$, from group k, $1 \leq k \leq Q$. To be able to recover a_i, any data item in group k cannot be used, so at least one item from another group is required to create the checksum, and this generates one additional checksum item. Therefore for all items in group k, $\lceil \frac{N}{Q} \rceil$ checksum items are generated so that any item in group k can be recovered. □

Applying this theorem, we have the following checksum algorithm: Suppose Q processes are in a process column or row, and let each process have K blocks of data of size $nb \times nb$. Without loss of generality, let K be the largest number of blocks owned by any of the Q processes. From Theorem 4.3, the size of the checksum in this row is K blocks.

Let C_i be the i^{th} checksum item, and A_i^j, be the i^{th} data item on process j, $1 \leq i \leq \lceil \frac{N}{Q} \rceil$, $1 \leq j \leq Q$:

$$C_k = \sum_{k=1}^{Q} A_k^k \tag{8}$$

Under (8), we have the following corollary:

Corollary 4.4. *The i^{th} block of checksum is calculated using the i^{th} block of data of each process having at least i blocks.*

4.5.2 Checksum Duplicates

Since ABFT checksum is stored by regular processors, it has to be considered as fragile as the matrix data. From Theorem 4.3 and using the same N and Q, the total number of checksum blocks is $K = \lceil \frac{N}{Q} \rceil$. These checksum blocks can be appended to the bottom or to the right of the global data matrix accordingly, and since checksum is stored on computing processes, these K checksum blocks are distributed over $\min(K, Q)$ processes (see Figure 3). If a failure strikes any of these processes, like (1, 0) in this example, some checksum is lost and cannot be recovered. Therefore, checksum itself needs protection; in our work, duplication is used to protect checksum from failure.

A straightforward way of performing duplication is to make a copy of the entire checksum block, as illustrated by the two rightmost columns in Figure 3. While simple to implement, this method suffers from two major defects. First, if the checksum width K is a multiple of Q (or P for column checksum), the duplicate of a checksum block is located on the same processors, defeating the purpose of duplication. This can be solved at the cost of introducing an extra empty column in the process grid to resolve the mapping conflict. More importantly, to maintain the checksum invariant property, it is required to apply the trailing matrix update on the checksum (and its duplicates) as well. From corollary 4.4, once all the i^{th} block columns on each process have finished the panel factorization (in Q step), the i^{th} checksum block column is no longer active in any further computation (except pivoting) and

should be excluded from the computing scope to reduce the ABFT overhead. This is problematic, as splitting the PBLAS calls to avoid excluded columns has a significant impact on the trailing matrix update efficiency.

4.5.3 Reverse Neighboring Checksum Storage

With the observation of how checksum is maintained during factorization, we propose the following reverse neighboring checksum duplication method that allows for applying the update in a single PBLAS call without incurring extraneous computation.

Algorithm 1 Checksum Management

On a $P \times Q$ grid, matrix is $M \times N$, block size is $NB \times NB$
C_k represents the k^{th} checksum block column
A_k represents the k^{th} data block column
Before factorization:
Generate the initial checksum:
$C_k = \sum_{j=(k-1)\times Q+1}^{(k-1)\times Q+Q} A_j, k = 1, \cdots, \left\lceil \frac{N}{NB\times Q} \right\rceil$
For each of C_k, make a copy of the whole block column and put right next to its original block column
Checksum C_k and its copy are put in the k^{th} position starting from the far right end
Begin factorization
Host algorithm starts with an initial scope of M rows and $N + \left\lceil \frac{N}{Q} \right\rceil$ columns
For each Q panel factorizations, the scope decreases M rows and $2 \times NB$ columns
End factorization

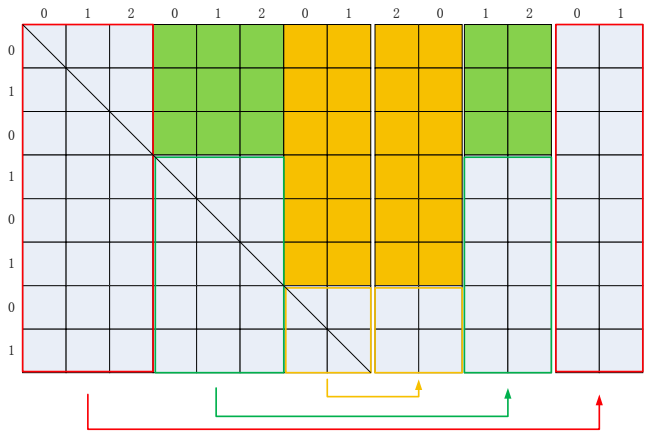

Figure 4. Reverse neighboring checksum storage, with two checksum duplicates per Q-wide groups

Figure 4 is an example of the reverse neighboring checksum method on a 2×3 grid. The data matrix has 8×8 blocks and therefore the size of checksum is 8×3 blocks with an extra 8×3 blocks copy. The arrows indicate where checksum blocks are stored on the right of the data matrix, according to the reverse storage scheme. For example, in the LU factorization, the first 3 block columns produce the checksum in the last two block columns (hence making 2 duplicate copies of the checksum). Because copies are stored in consecutive columns of the process grid, for any 2D grid with $Q > 1$, the checksum duplicates are guaranteed to be stored on different processors. The triangular solve (TRSM) and trailing matrix update (GEMM) are applied to the whole checksum area until the first three columns are factored. In following factorization steps, the two last block columns of checksum are excluded from the TRSM and GEMM scope. Since TRSM and GEMM claim most of the computation in the LU factorization, this shrinking scope greatly reduces the overhead of the ABFT mechanism. One can note that only the upper part of the checksum is useful, we will explain in the next section how this extra storage can be used to protect the lower triangular part of the matrix.

4.6 Delayed Recovery and Error Propagation

In this work, we assume that a failure can strike at any moment during the life span of factorization operations or even the recovery process. Theorem 4.2 proves that at the moment where the failure happens, the checksum invariant property is satisfied, meaning that the recovery can proceed successfully. However, in large scale systems, which are asynchronous by nature, the time interval between the failure and the moment when it is detected by other processes is unknown, leading to delayed recoveries, with opportunities for error propagation.

The ZU factorization is composed of several sub-algorithms that are called on different parts of the matrix. Matrix multiplication, which is used for trailing matrix updates and claims more than 95% of the execution time, has been shown to be ABFT compatible [4] , that is to compute the correct result even with delayed recovery. One feature that has the potential to curb this compatibility is pivoting, in LU, especially when a failure occurs between the panel factorization and the row swapping updates, there is a potential for destruction of rows in otherwise unaffected blocks.

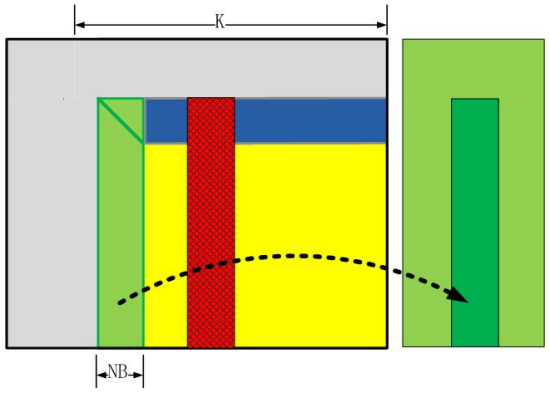

Figure 5. Ghost pivoting Issue
Gray: Result in previous steps
Light Green: Panel factorization result in current step
Deep Green: The checksum that protects the light green
Blue: TRSM zone Yellow: GEMM zone
Red: one of the columns affected by pivoting

Figure 5 shows an example of such a case. Suppose the current panel contributes to the i^{th} column of checksum. When panel factorization finishes, the i^{th} column becomes intermediate data which does not cover any column of matrix. If a failure at this instant causes holes in the current panel area, then lost data can be recovered right away. Pivoting for this panel factorization has only been applied within the light green area. Panel factorization is repeated to continue on the rest of the factorization. However, if failure causes holes in other columns that also contribute to the i^{th} column of checksum, these holes cannot be recovered until the end of the trailing matrix update. To make it worse, after the panel factorization, pivoting starts to be applied outside the panel area and can move rows in holes into healthy area or vice versa,

extending the recovery area to the whole column, as shown in red in Figure 5 including triangular solving area. To recover from this case, in addition to matrix multiplication, the triangular solver is also required to be protected by ABFT.

Theorem 4.5. *Failure in the right-hand sides of triangular solver can recover from fail-stop failure using ABFT.*

Proof. Suppose A is the upper or lower triangular matrix produced by LU factorization (non-blocked in ScaLAPACK LU), B is the right-hand side, and the triangular solver solves the equation $Ax = B$.

Supplement B with checksum generated by $B_c = B * G_r$ to extended form $\hat{B} = [B,\ B_c]$, where G_r is the generator matrix. Solve the extended triangular equation:

$$\begin{aligned} Ax_c &= B_c = [B,\ B_c] \\ \therefore\ x_c &= A^{-1} \times [B,\ B_c] \\ &= \left[A^{-1}B,\ A^{-1}B_c\right] \\ &= \left[x,\ A^{-1}BG_r\right] \\ &= [x,\ xG_r] \end{aligned}$$

Therefore data in the right-hand sides of the triangular solver is protected by ABFT. □

With this theorem, if failure occurs during triangular solving, lost data can be recovered when the triangular solver completes. Since matrix multiplication is also ABFT compatible, the whole red region in Figure 5 can be recovered after the entire trailing matrix update is done, leaving the opportunity for failure detection and recovery to be delayed at a convenient moment in the algorithm.

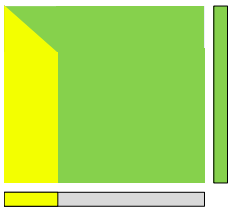

Figure 6. Separation of lower and upper areas protected by checksum (green) and checkpoint (yellow) during the course of the factorization algorithm

5. Protection of the Left Factor Matrix with Q-parallel Checkpoint

It has been proven in Theorem 4.2 that the checksum only covers the upper triangular part of the matrix until the current panel, and the trailing matrix is subject to future updates. This is depicted in Figure 6, where the green checksum on the right of the matrix protects exclusively the green part of the matrix. Another mechanism must be added for the protection of the left factor (the yellow area).

5.1 Impracticability of ABFT for Left Factor Protection

The most straightforward idea, when considering the need of protecting the lower triangle of the matrix, is to use an approach similar to the one described above, but column-wise. Unfortunately, such an approach is difficult, if not impossible in some cases, as proved in the remaining of this Section.

5.1.1 Pivoting and Vertical Checksum Validity

In LU, partial pivoting prevents the left factor from being protected through ABFT. The most immediate reason is as follow: The PBLAS kernel used to compute the panel factorization (see Figure 1) performs simultaneously the search for the best pivot in the column and the scaling of the column with that particular pivot. If applied directly on the matrix and the checksum blocks, similarly to what the trailing update approach does, checksum elements are at risk of being selected as pivots, which results in exchanging checksum rows into the matrix. This difficulty could be circumvented by introducing a new PBLAS kernel that does not search for pivots in the checksum.

Unfortunately, legitimate pivoting would still break the checksum invariant property, due to row swapping. In LU, for matrix A,

$$\begin{aligned} A &= \begin{pmatrix} A_{11} & A_{12} \\ A_{21} & A_{22} \end{pmatrix} = \begin{pmatrix} L_{11} & 0 \\ L_{21} & L_{22} \end{pmatrix} \begin{pmatrix} U_{11} & U_{12} \\ 0 & U_{22} \end{pmatrix} \\ &= \begin{pmatrix} L_{11}U_{11} & L_{11}U_{12} \\ L_{21}U_{11} & L_{21}U_{12} + L_{22}U_{22} \end{pmatrix} \end{aligned} \tag{9}$$

Panel factorization is:

$$\begin{pmatrix} A_{11} \\ A_{21} \end{pmatrix} = \begin{pmatrix} L_{11}U_{11} \\ L_{21}U_{11} \end{pmatrix} = \begin{pmatrix} L_{11} \\ L_{21} \end{pmatrix} U_{11} \tag{10}$$

To protect L_{11} and L_{21}, imagine that we maintain a separate checksum, stored at the bottom of the matrix, as shown in the yellow bottom rectangle of Figure 6, that we plan on updating by scaling it accordingly to the panel operation. In this vertical checksum, each P tall group of blocks in the 2D block cyclic distribution is protected by a particular checksum block. Suppose rows i_1 and i_2 reside on blocks k_{i_1} and k_{j_1} of two processes. It is not unusual that $k_{i_1} \neq k_{j_1}$. By Corollary 4.4, block k_{i_1} and k_{j_1} contribute to column-wise checksum block k_{i_1} and k_{j_1} respectively in the column that local blocks k_{i_1} and k_{j_1} belong to. This relationship is expressed as

$$\begin{aligned} row\ i_1 &\mapsto checksum\ block\ k_{i_1} \\ row\ j_1 &\mapsto checksum\ block\ k_{j_1} \end{aligned}$$

$\mapsto$ reads 'contributes to'. After the swapping, the relationship should be updated to

$$\begin{aligned} row\ i_1 &\mapsto checksum\ block\ k_{j_1} \\ row\ j_1 &\mapsto checksum\ block\ k_{i_1} \end{aligned}$$

This requires a re-generation of checksum blocks k_{i_1} and k_{j_1} in order to maintain the checkpoint validity. Considering there are nb potential pivoting operations per panel, hence a maximum of $nb+1$ checksum blocks to discard, this operation has the potential to be as expensive as computing a complete vertical checkpoint.

5.1.2 QR Factorization

Although QR has no pivoting, it still cannot benefit from ABFT to cover Q, as we prove below.

Theorem 5.1. *Q in Householder QR factorization cannot be protected by performing factorization along with the vertical checksum.*

Proof. Append a $m \times n$ nonsingular matrix A with checksum GA of size $c \times n$ along the column direction to get matrix $A_c = \begin{bmatrix} A \\ GA \end{bmatrix}$. G is $c \times m$ generator matrix. Suppose A has a QR factorization $Q_0 R_0$.

Perform QR factorization to A_c:

$$\begin{bmatrix} A \\ GA \end{bmatrix} = Q_c R_c = \begin{bmatrix} Q_{c11} & Q_{c12} \\ Q_{c21} & Q_{c22} \end{bmatrix} \begin{bmatrix} R_{c11} \\ \varnothing \end{bmatrix}$$

Q_{c11} is $m \times m$ and Q_{c21} is $c \times m$. R_c is $m \times n$ and $\varnothing$ represents $c \times n$ zero matrix. $R_c \neq 0$ and is full rank. Because R_c is upper triangular with nonzero diagonal elements and therefore nonsingular.

$$Q_c Q_c^T = \begin{bmatrix} Q_{c11} & Q_{c12} \\ Q_{c21} & Q_{c22} \end{bmatrix} \begin{bmatrix} Q_{c11}^T & Q_{c21}^T \\ Q_{c12}^T & Q_{c22}^T \end{bmatrix} = I$$

Therefore

$$Q_{c11} Q_{c11}^T + Q_{c12} Q_{c12}^T = I. \tag{11}$$

Since $A = Q_{c11} R_{c11}$ and R_{c11} is nonsingular, then $Q_{c11} \neq 0$ and nonsingular.

Assume $Q_{c12} = 0$:

$Q_{c11} Q_{c21}^T + Q_{c12} Q_{c22}^T = 0$, therefore $Q_{c11} Q_{c21}^T = 0$. We have shown that Q_{c11} is nonsingular, so $Q_{c21}^T = 0$ and this conflicts with $GA = Q_{c21} R_{c11} \neq 0$, so the assumption $Q_{c12} = 0$ does not hold. From Equation 11, $Q_{c11} Q_{c11}^T \neq I$. This means even though $A = Q_{c11} R_{c11}$, $Q_{c11} R_{c11}$ is not a QR factorization of A. □

5.2 Panel Checkpointing

Given that the ZU factorization cannot protect Z by applying ABFT in the same way as for U, separate efforts are needed. For the rest of this paper, we use the term "checksum" to refer to the ABFT checksum, generated before the factorization, that is maintained by the application of numerical updates during the course of the algorithm, in contrast to "checkpointing" for the operation that creates a new protection block during the course of the factorization. LU factorization with partial pivoting being the most complex problem, it is used here for the discussion. The method proposed in this section can be applied to the QR and Cholesky factorizations with minimal efforts nonetheless.

In a ZU block factorization using 2D cyclic distribution, once a panel of Z is generated, it is stored into the lower triangular region of the original matrix. For example, in LU, vectors of L, except the diagonal ones, are stored in L. These lower triangular parts from the panel factorization are final results, and are not subject to further updates during the course of the algorithm, except for partial pivoting row swapping in LU. Therefore only one vertical checkpointing *"should be"* necessary to maintain each panel's safety, as is discussed in [12]. We will show how this idea, while mathematically trivial, needs to be refined to support partial pivoting. We will then propose a novel checkpointing scheme, leveraging properties of the block algorithm to checkpoint Z in parallel, that demonstrates a much lower overhead when compared to this basic approach.

5.3 Postponed Left Pivoting

Although once a panel is factored, it is not changed until the end of the computation, row swaps incurred by pivoting are still to be applied to the left factor as the algorithm progresses in the trailing matrix, as illustrated in Figure 1. The second step (pivoting to the left) swaps two rows to the left of the current panel. The same reasoning as presented in section 5.1.1 holds, meaning that the application of pivoting row swaps to the left factor has the potential to invalidate checkpoint blocks. Since pivoting to the left is carried out in every step of LU, this causes significant checkpoint maintenance overhead.

Unlike pivoting to the right, which happens during updates and inside the panel operation, whose result are reused in following steps of the algorithm, pivoting to the left can be postponed. The factored L is stored in the lower triangular part of the matrix without further usage during the algorithm. As a consequence, we delay the application of all left pivoting to the end of the computation, in order to avoid expensive checkpoint management. We keep track of all pivoting that should have been applied to the left factor, and when the algorithm has completed, all row swaps are applied just in time before returning the end-result of the routine.

5.4 Q-Parallel Checkpointing of Z

The vertical checkpointing of the panel result requires a set of reduction operations immediately after each panel factorization. Panel factorization is on the critical path and has lower parallelism, compared to other routines of the factorization (such as trailing matrix update). The panel factorization works only on a single block column of the matrix, hence benefits from only a P degree of parallelism, in a $P \times Q$ process grid. Checkpointing worsens this situation, because it applies to the same block column, and is bound to the same low level of exploitable parallelism. Furthermore, the checkpointing cannot be overlapped with the computation of the trailing matrix update: all processes who do not appear on the same column of the process grid are waiting in the matrix-matrix multiply PBLAS, stalled because they require the panel column to enter the call in order for the result of the panel to be broadcasted. If the algorithm enters the checkpointing routine before going into the trailing update routine, the entire update is delayed. If the algorithm enters the trailing update before starting the checkpointing, the checksum is damaged in a way that prevents recovering that panel, leaving it vulnerable to failures.

Our proposition is then twofold: we protect the content of the blocks before the panel, which then enables starting immediately the trailing update without jeopardizing the safety of the panel result. Then, we wait until sufficient checkpointing is pending to benefit from the maximal parallelism allowed by the process grid.

5.4.1 Enabling Trailing Matrix Update Before Checkpointing

The major problem with enabling the trailing matrix update to proceed while the checkpointing of the panel is not finished is that the ABFT protection of the update modifies the checksum in a way that disables protection for the panel blocks. To circumvent this limitation, in a $P \times Q$ grid, processes are grouped by section of width Q, that are called a *panel scope*. When the panel operation starts applying to a new section, the processes of this panel scope make a local copy of the impending column and the associated checksum, called a *snapshot*. This operation involves no communication, and features the maximum $P \times Q$ parallelism. The memory overhead is limited, as it requires only the space for at most two extra columns to be available at all time, one for saving the state before the application of the panel to the target column, and one for the checksum column associated to these Q columns. The algorithm then proceeds as usual, without waiting for checkpoints before entering the next Q trailing updates. Because of the availability of this extra protection column, the original checksum can be modified to protect the trailing matrix without threatening the recovery of the panel scope, which can rollback to that previous dataset should a failure occur.

5.4.2 Q-Parallel Checkpointing

When a panel scope is completed, the $P \times Q$ group of processes undergo checkpointing simultaneously. Effectively, P simultaneous checkpointing reductions are taking place along the block rows, involving the Q processes of that row to generate a new protection block. This scheme enables the maximum parallelism for the checkpoint operation, hence decreasing its global impact on the failure free overhead. Another strong benefit is that it scales with the process grid perfectly, whereas regular checkpointing suffers from scaling with the square root of the number of processes (as it involves only one dimension of the process grid).

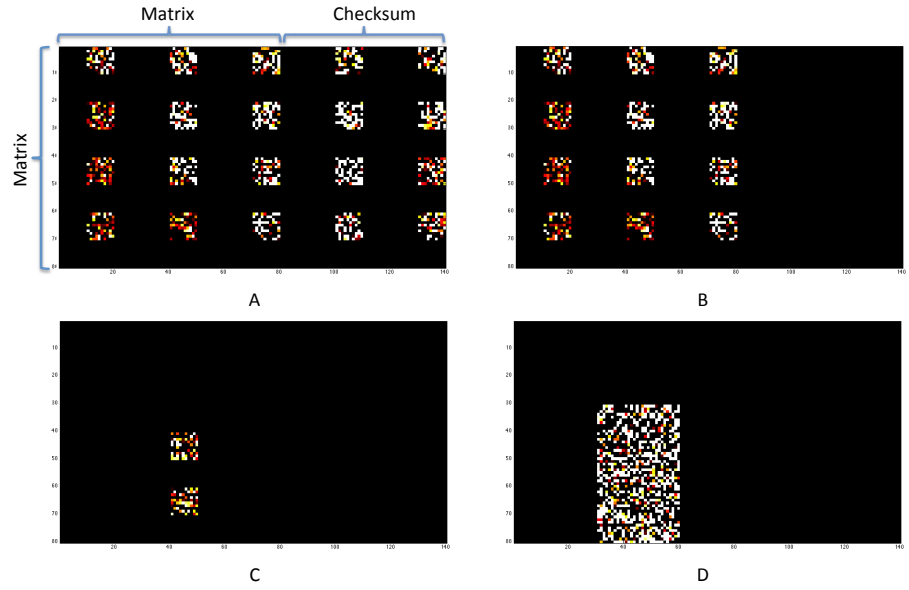

Figure 7. Recovery example
(matrix size 800×800, grid size 2×3, failure of process (0,1), failure step:41,
A: Failure occurs B: Checksum recovered
C: Data recovered using ABFT checksum and checkpointing output D: Three panels restored using snapshots

5.4.3 Optimized Checkpoint Storage

According to Corollary 4.4, starting from the first block column on the left, every Q block columns contribute to one block column of checksum, which means that once the factorization is done for these Q block columns, the corresponding checksum block column becomes useless (it does not protect the trailing matrix anymore, it has never protected the left factor, see Theorem 4.2). Therefore, this checksum storage space is available for storing the resultant checkpoint block generated to protect the panel result. Following the same policy as the checksum storage, discussed in Section 4.5.2, the checkpoint data is stored in reverse order from the right of the checksum (see Figure 4). As this part of the checksum is excluded from the trailing matrix update, the checkpoint blocks are not modified by the continued operation of the algorithm.

5.4.4 Recovery

The hybrid checkpointing approach requires a special recovery algorithm. Two cases are considered. First, when failure strikes during the trailing update, immediately after a panel scope checkpointing. For this case, the recovery is not attempted until the current step of the trailing update is done. When the recovery time comes, the checksum/checkpointing on the right of the matrix matches the matrix data as if the initial ABFT checksum had just been performed. Therefore any lost data blocks can be recovered by the simple reverse application of the ABFT checksum relationship.

The second case is when a failure occurs during the Q panel factorization, before the checkpointing for this panel scope can successfully finish. In this situation, all processes revert the panel scope columns to the snapshot copy. Holes in the snapshot data are recreated by using the snapshot copy of the checksum, applying the usual ABFT recovery. The algorithm is resumed in the panel scope, so that panel and updates are applied again within the scope of the Q wide section; updates outside the panel scope are discarded, until the pre-failure iteration has been reached. Outside the panel scope, regular recovery mechanisms are deployed (ABFT checksum inversion for the trailing matrix, checkpoint recovery for the left factor). When the re-factorization of panels finishes, the entire matrix, including the checksum, is recovered back to the correct state. The computation then resumes from the next panel factorization, after the failing step.

Figure 7 shows an example of the recovery when the process (1,0) in a 2×3 grid failed. It presents the difference between the correct matrix dataset and the current dataset during various steps of failure recovery as a "temperature map", brighter colors meaning large differences and black insignificant differences. The matrix size is 80×80 and $NB = 10$, therefore the checksum size is 80×60. Failure occurs after the panel factorization starting at (41,41) is completed, within the $Q = 3$ panel scope. First, using a fault tolerant MPI infrastructures, like FT-MPI [15], the failed process (0,1) is replaced and reintegrates the process grid with a blank dataset, showing as evenly distributed erroneous blocks (A). Then the recovery process starts by mending the checksum using duplicates (B). The next step recovers the data which is outside the current panel scope (31:80,31:60), using the corresponding checksum for the right factor, and the checkpoints for the left factor (C). At this moment, all the erroneous blocks are repaired, except those in the panel scope (41:80, 41:50). Snapshots are applied to the three columns of the panel scope (31:80,31:60). Since these do not match the state of the matrix before the failure, but a previous state, this area appears as very different (D). Panel factorization is re-launched in the panel scope, in the area (31:80,31:60), with the trailing update limited within this area. This re-factorization continues until it finishes panel (41:80,41:50) and by that time the whole matrix is recovered to the correct state (not presented, all black). The LU factorization can then proceed normally.

6. Evaluation

In this section, we evaluate the performance of the proposed fault tolerant algorithm based on ABFT and reverse neighboring checkpointing. For a fault tolerant algorithm, the most important consid-

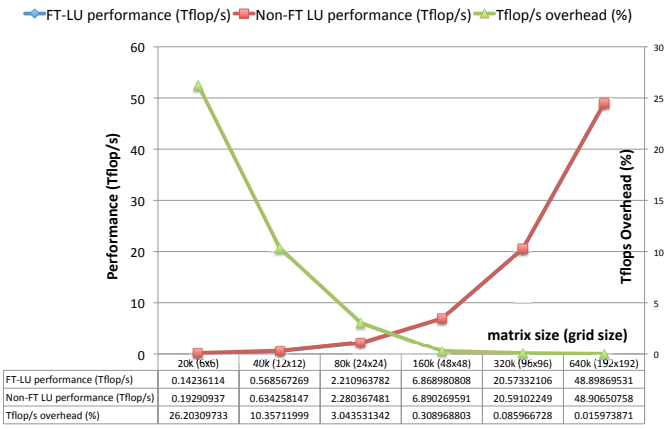

	20k (6x6)	40k (12x12)	80k (24x24)	160k (48x48)	320k (96x96)	640k (192x192)
FT-LU performance (Tflop/s)	0.14236114	0.568567269	2.210963782	6.868980808	20.57332106	48.89869531
Non-FT LU performance (Tflop/s)	0.19290937	0.634258147	2.280367481	6.890269591	20.59102249	48.90650758
Tflop/s overhead (%)	26.20309733	10.35711999	3.043531342	0.308968803	0.085966728	0.015973871

Figure 8. Weak scalability of FT-LU: performance and overhead on Kraken, compared to non fault tolerant LU

FT overhead (Tflop/s)	0.051	0.066	0.070	0.021	0.018	0.008
FT overhead (%)	26.203	10.357	3.044	0.309	0.086	0.016

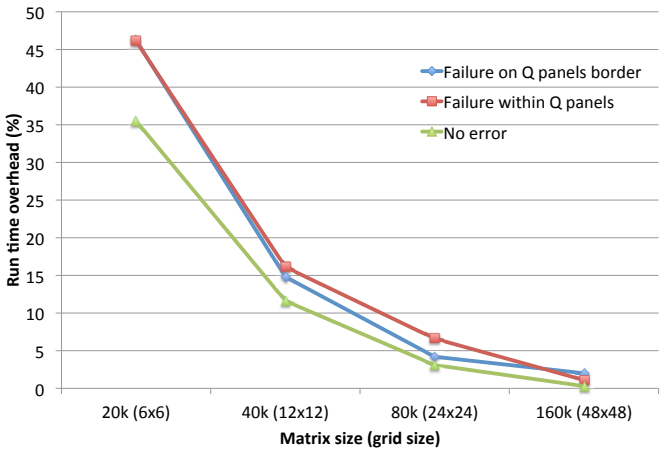

Figure 9. Weak scalability of FT-LU: run time overhead on Kraken when failures strike at different steps

eration is the overhead added to failure free execution rate, due to various fault tolerance mechanisms such as checksum generation, checkpointing and extra flops. An efficient and scalable algorithm will incur a minimal overhead over the original algorithm while enabling scalable reconstruction of lost dataset in case of failure.

We use the NSF Kraken supercomputer, hosted at the National Institute for Computational Science (NICS, Oak Ridge, TN) as our testing platform. This machine features 112,896 2.6GHz AMD Opteron cores, 12 cores per node, with the Seastar interconnect. At the software level, to serve as a comparison base, we use the non fault tolerant ScaLAPACK LU and QR in double precision with block size $NB = 100$. The fault tolerance functions are implemented and inserted as drop-in replacements for ScaLAPACK routines.

In this section, we first evaluate the storage overhead in the form of extra memory usage, then show experimental result on Kraken to assess the computational overhead.

6.1 Storage Overhead

Checksum takes extra storage (memory), but on large scale systems, memory usage is usually maximized for computing tasks. Therefore, it is preferable to have a small ratio of checksum size over matrix size, in order to minimize the impact on the memory available to the application itself. For the sake of simplicity, and because of the small impact in term of memory usage, neither the pivoting vector nor the column shift are considered in this evaluation.

Different protection algorithms require different amounts of memory. In the following, we consider the duplication algorithm presented in Section 4.5.2 for computing the upper memory bound. The storage of the checksum includes the row-wise and column-wise checksums and a small portion at the bottom-right corner.

For an input matrix of size $M \times N$ on a $P \times Q$ process grid, the memory used for checksum (including duplicates) is $M \times \frac{N}{Q} \times 2$. The ratio R_{mem} of checksum memory over the memory of the input matrix, equals to $\frac{2}{Q}$, becomes negligible with the increase in the number of processes used for the computation.

6.2 Overhead without Failures

Figure 8 evaluates the completion time overhead and performance, using the LU factorization routine PDGETRF. The performance of both the original and fault tolerant version are presented, in Tflop/s (the two curves overlap due to the little performance difference). This experiment is carried out to test the weak scalability, where both the matrix and grid dimension doubles. The result outlines that as the problem size and grid size increases, the overhead drops quickly and eventually becomes negligible. At the matrix size of $640,000 \times 640,000$, on $36,864$ (192×192) cores, both versions achieved over 48Tflop/s, with an overhead of 0.016% for the ABFT algorithm. As a side experiment, we implemented the naive vertical checkpointing method discussed in section 5.2, and as expected the measured overhead quickly exceeds 100%.

As the left factor is touched only once during the computation, the approach of checkpointing the result of a panel synchronously can, *a-priori*, look sound when compared to system based checkpoint, where the entire dataset is checkpointed periodically. However, as the checkpointing of a particular panel suffers from its inability to exploit the full parallelism of the platform, it is subject to a derivative of Amdahl's law, its parallel efficiency is bound by P, while the overall computation enjoys a $P \times Q$ parallel efficiency: its importance is bound to grow when the number of computing resources increases. As a consequence, in the experiments, the time to compute the naive checkpoint dominates the computation time. On the other hand, the hybrid checkpointing approach exchanges the risk of a Q-step rollback with the opportunity to benefit from a $P \times Q$ parallel efficiency for the panel checkpointing. Because of this improved parallel efficiency, the hybrid checkpointing approach benefits from a competitive level of performance, that follows the same trend as the original non fault tolerant algorithm.

6.3 Recovery Cost

In addition to the "curb" overhead of fault tolerance functions, the recovery from failure adds extra overhead to the host algorithm. There are two cases for the recovery. The first one is when failure occurs right after the reverse neighboring checkpointing of Q panels. At this moment the matrix is well protected by the checksum and therefore the lost data can be recovered directly from the checksum. We refer to this case as "failure on Q panels border". The second case is when the failure occurs during the reverse neighboring checkpointing and therefore local snapshots have to be used along with re-factorization to recover the lost data and restore the matrix state. This is referred to as the "failure within Q panels".

Figure 9 shows the overhead from these two cases for the LU factorization, along with the no-error overhead as a reference. In the "border" case, the failure is simulated to strike when the 96^{th} panel (which is a multiple of grid columns, $6, 12, \cdots, 48$) has

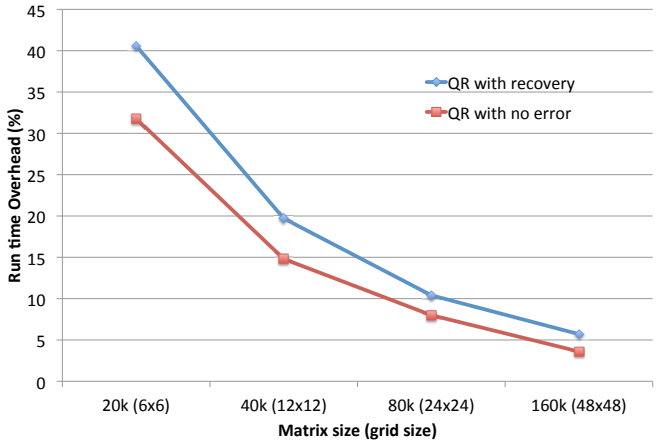

Figure 10. Weak scalability of FT-QR: run time overhead on Kraken when failures strike

just finished. In the "non-border" case, failure occurs during the $(Q+2)^{th}$ panel factorization. For example, when $Q = 12$, the failure is injected when the trailing update for the step with panel (1301,1301) finishes. From the result in Figure 9, the recovery procedure in both cases adds a small overhead that also decreases when scaled to large problem size and process grid. For largest setups, only 2-3 percent of the execution time is spent recovering from a failure.

6.4 Extension to Other factorization

The algorithm proposed in this work can be applied to a wide range of dense matrix factorizations other than LU. As a demonstration we have extended the fault tolerance functions to the ScaLAPACK QR factorization in double precision. Since QR uses a block algorithm similar to LU (and also similar to Cholesky), the integration of fault tolerance functions is mostly straightforward. Figure 10 shows the performance of QR with and without recovery. The overhead drops as the problem and grid size increase, although it remains higher than that of LU for the same problem size. This is expected: as the QR algorithm has a higher complexity than LU ($\frac{4}{3}N^3$ v.s. $\frac{2}{3}N^3$), the ABFT approach incurs more extra computation when updating checksums. Similar to the LU result, recovery adds an extra 2% overhead. At size 160,000 a failure incurs about 5.7% penalty to be recovered. This overhead becomes lower, the larger the problem or processor grid size considered.

7. Conclusion

In this paper, by assuming a failure model in which fail-stop failures can occur anytime on any process during a parallel execution, a general scheme of ABFT algorithms for protecting one-sided matrix factorizations is proposed. This scheme can be applied to a wide range of dense matrix factorizations, including Cholesky, LU and QR. A significant property of the proposed algorithms is that both the left and right factorization results are protected. ABFT is used to protect the right factor with checksum generated before, and carried along during the factorizations. A highly scalable checkpointing method is proposed to protect the left factor. This method cooperatively reutilizes the memory space originally designed to store the ABFT checksum, and has minimal overhead by strategically coalescing checkpoints of many iterations. Large scale experimental results validate the design of the proposed fault tolerance method by highlighting scalable performance and decreasing overhead for both LU and QR. In the future this work will be extended to support multiple simultaneous failures.

References

[1] Fault tolerance for extreme-scale computing workshop report, 2009.

[2] http://www.top500.org/, 2011.

[3] L. Blackford, A. Cleary, J. Choi, E. D'Azevedo, J. Demmel, I. Dhillon, J. Dongarra, S. Hammarling, G. Henry, A. Petitet, et al. *ScaLAPACK users' guide*. Society for Industrial Mathematics, 1997.

[4] G. Bosilca, R. Delmas, J. Dongarra, and J. Langou. Algorithm-based fault tolerance applied to high performance computing. *Journal of Parallel and Distributed Computing*, 69(4):410–416, 2009.

[5] A. Bouteiller, G. Bosilca, and J. Dongarra. Redesigning the message logging model for high performance. *Concurrency and Computation: Practice and Experience*, 22(16):2196–2211, 2010.

[6] G. Burns, R. Daoud, and J. Vaigl. LAM: An open cluster environment for MPI. In *Proceedings of SC'94*, volume 94, pages 379–386, 1994.

[7] F. Cappello. Fault tolerance in petascale/exascale systems: Current knowledge, challenges and research opportunities. *International Journal of High Performance Computing Applications*, 23(3):212, 2009.

[8] Z. Chen and J. Dongarra. Algorithm-based checkpoint-free fault tolerance for parallel matrix computations on volatile resources. In *IPDPS'06*, pages 10–pp. IEEE, 2006.

[9] Z. Chen and J. Dongarra. *Scalable techniques for fault tolerant high performance computing*. PhD thesis, University of Tennessee, Knoxville, TN, 2006.

[10] Z. Chen and J. Dongarra. Algorithm-based fault tolerance for fail-stop failures. *IEEE TPDS*, 19(12):1628–1641, 2008.

[11] J. Choi, J. Demmel, I. Dhillon, J. Dongarra, S. Ostrouchov, A. Petitet, K. Stanley, D. Walker, and R. Whaley. ScaLAPACK: a portable linear algebra library for distributed memory computers–design issues and performance. *Computer Physics Comm.*, 97(1-2):1–15, 1996.

[12] T. Davies, C. Karlsson, H. Liu, C. Ding, , and Z. Chen. High Performance Linpack Benchmark: A Fault Tolerant Implementation without Checkpointing. In *Proceedings of the 25th ACM International Conference on Supercomputing (ICS 2011)*. ACM.

[13] J. Dongarra, L. Blackford, J. Choi, A. Cleary, E. D'Azevedo, J. Demmel, I. Dhillon, S. Hammarling, G. Henry, A. Petitet, et al. ScaLAPACK user's guide. *Society for Industrial and Applied Mathematics, Philadelphia, PA*, 1997.

[14] E. Elnozahy, D. Johnson, and W. Zwaenepoel. The performance of consistent checkpointing. In *Reliable Distributed Systems, 1992. Proceedings., 11th Symposium on*, pages 39–47. IEEE, 1991.

[15] G. Fagg and J. Dongarra. FT-MPI: Fault tolerant MPI, supporting dynamic applications in a dynamic world. *EuroPVM/MPI*, 2000.

[16] G. Gibson. Failure tolerance in petascale computers. In *Journal of Physics: Conference Series*, volume 78, page 012022, 2007.

[17] G. Golub and C. Van Loan. *Matrix computations*. Johns Hopkins Univ Pr, 1996.

[18] D. Hakkarinen and Z. Chen. Algorithmic Cholesky factorization fault recovery. In *Parallel & Distributed Processing (IPDPS), 2010 IEEE International Symposium on*, pages 1–10. IEEE, 2010.

[19] K. Huang and J. Abraham. Algorithm-based fault tolerance for matrix operations. *Computers, IEEE Transactions on*, 100(6):518–528, 1984.

[20] V. Kumar, A. Grama, A. Gupta, and G. Karypis. *Introduction to parallel computing: design and analysis of algorithms*, volume 400. Benjamin/Cummings, 1994.

[21] C. Lu. *Scalable diskless checkpointing for large parallel systems*. PhD thesis, Citeseer, 2005.

[22] F. Luk and H. Park. An analysis of algorithm-based fault tolerance techniques* 1. *Journal of Parallel and Distributed Computing*, 5(2):172–184, 1988.

[23] J. Plank, K. Li, and M. Puening. Diskless checkpointing. *Parallel and Distributed Systems, IEEE Transactions on*, 9(10):972–986, 1998.

[24] F. Streitz, J. Glosli, M. Patel, B. Chan, R. Yates, B. Supinski, J. Sexton, and J. Gunnels. Simulating solidification in metals at high pressure: The drive to petascale computing. In *Journal of Physics: Conference Series*, volume 46, page 254. IOP Publishing, 2006.